Astrometric Modeling for the Space Interferometry Mission

Mark H. Milman[a] and Slava G. Turyshev[b]

Jet Propulsion Laboratory, California Institute of Technology, Pasadena, CA 91109

ABSTRACT

The Space Interferometry Mission (SIM) is a space-based long-baseline optical interferometer for precision astrometry. One of the primary objectives of the SIM instrument is to accurately determine the directions to a grid of stars, together with their proper motions and parallax, improving a priori knowledge by nearly three orders of magnitude. The SIM instrument does not directly measure the angular separation between stars, but the projection of each star direction vector onto the interferometer baseline vector by measuring the pathlength delay of starlight as it passes through the two arms of the interferometer. Because the a priori baseline vector is only known to arcsec accuracy through on-board attitude information, the interferometer baseline vector must also be estimated in an *a posteriori* manner in addition to the astrometric parameters. A consequence of this is that in order to generate a consistent set of equations from which to determine the astrometric parameters, multiple measurements of each star with different baseline orientations must be made, and dually multiple star measurements must be made with each baseline.

SIM makes the pathlength delay measurement by a combination of internal metrology measurements to determine the distance the starlight travels through the two arms of the interferometer and a measurement of the white light stellar fringe to find the point of equal pathlength. Because this operation requires a non–negligible integration time to accumulate enough photons to measure the stellar fringe position, the baseline vector is not stationary over this time period as its absolute length and orientation are time–varying. This conflicts with the requirement that a single baseline vector measures a set of stars. This paper addresses how the time-varying baseline is "regularized" so that it may act as a single baseline vector for multiple stars. The notion of the regularized baseline is fundamental to the extraction of the astrometric parameters. It has been used extensively in a number of grid simulation studies to plan observation sequences for the mission, etc. We present theory of guide interferometers angle feedforward and discuss implications for the SIM instrument design and simulations.

Keywords: SIM, metrology, pathlength and angle feedforward, astrometry, modeling

1. INTRODUCTION

As an integral part of its function, the Space Interferometry Mission (SIM) will initialize and maintain a full-sky astrometric model of a set of objects. This model is known as the astrometric grid. The grid serves as the astrometric calibration for the SIM instrument, and is essential to support the wide-angle astrometric science goals for the SIM mission.

Much of the astrometric science to be performed by SIM requires the measurement of the relative angle between two widely separated objects. For instance, the measurement of the absolute annual parallax for an object requires a measurement of its parallactic motion relative to objects roughly 90 degrees away. Because SIM's astrometric field of view (FOV) is necessarily much smaller than 90 degrees, this relative angular measurement cannot be made directly. To support such wide angle astrometry, SIM uses an astrometric grid of objects spanning the entire 4 π celestial sphere. Measurements are made on these grid objects, and their relative angular positions and motions are estimated in a process known as grid reduction. In these grid reductions a 4 π astrometric model for the grid objects (and various instrument parameters) is fit to the measurement set.

For local science experiments (within the SIM astrometric FOV), nearby grid objects represent (quasi-inertial) astrometric references that fix the spacecraft attitude and instrument calibration. For more global problems, the grid represents the truss work by which angles larger than the instrument FOV are spanned. Additionally, there will be serendipitous science that emerges from the grid solutions themselves, as grid solution position and motion estimates can probe several astrophysical and galactic structure issues directly - depending on our selection of grid constituents.

Further author information: (Send correspondence to S.G.T.)
M.H.M.: E-mail: Mark.Milman@jpl.nasa.gov
S.G.T.: E-mail: Slava.Turyshev@jpl.nasa.gov

2. SIM ASTROMETRIC OBSERVATIONS

Before discussing SIM grid observations, it is prudent to review the method by which SIM makes astrometric measurements. SIM is designed to measure the pathlength delay between the two arms of the interferometer as it is locked on the fringe of a single target object. This delay value is our astrometric observable, and it is measured by the internal metrology system of the interferometer. A sequence of observations consists of several such measurements, including target and reference stars as well as grid stars. The delay value is given formally by the interferometer astrometric equation:

$$d = (\vec{s} \cdot \vec{b}) + k + \epsilon \tag{1}$$

where d is the optical pathlength delay that is measured by the interferometer, $\vec{s}$ is the normal to the wavefront of the starlight (the unit 3-vector to the observed object), $\vec{b}$ is the baseline 3-vector, k is a so-called constant term that represents possible optical path differences between the light collected from the target object and the internal metrology, and ϵ is a noise term resulting from the finite accuracy of the internal metrology measurement. Both $\vec{B}b$ and k are assumed to remain constant within a sequence of observations. The delay measured for the grid stars, whose position is assumed known, is used to determine the baseline vector $\vec{b}$. The difference in measured delay between target and reference stars then is a measurement of their angular separation projected onto the baseline vector.

A variation in the average constant term, k, from tile-to-tile may have profound implications on the grid reduction accuracy. This can at least qualitatively be understood from the fact that in leading order a nonzero average value of the constant term amounts to a rotation of the baseline vector - thus the relative geometry of objects within the tile is unaffected. However, these results do not address the implications of the variation in the constant term within the observations contained in a tile. Such inner-tile k variation is potentially more significant, as it translates into a distortion of the relative geometry for the objects in the tile. The implications of inner-tile k variation on the grid reduction accuracy will be a subject of future study.

SIM surveys the sky in units that were named tiles. A tile is defined as sequence of measured delays corresponding to multiple objects all made by a single baseline vector B and central pointing of the instrument - that is all the measurements in a tile are from objects that are within a single astrometric FOV. The collection of such a measurement set with a single interferometer is literally impossible: the data collection on a sequence of objects takes finite time, over which both the baseline length and attitude will in general evolve in time. The implicit assumption here is that the combination of relative metrology and guide interferometer measurements are sufficient to reduce a sequence of delays made with the science interferometer into a virtual set of delays that correspond to the single baseline model. We shall call this reduction process regularization. Herein we assume regularization of the tile measurement set is possible. Through arguments made above, to be astrometrically useful a tile must contain four or more measurements.

Delay measurements of target and reference stars are taken at arbitrary times throughout the nominal mission lifetime (set to 5 years), and at arbitrary spacecraft orientations—neglecting possible visibility, orientation and planning constraints that might restrict the observing sequence. As each measurement is strictly one-dimensional, the necessary two-dimensional information required to fully determine the position of both science and reference objects is obtained by making observations at successive epochs with orthogonal orientations of the baseline vector $\vec{b}$. A *full astrometric observation* of a target is the set of delay measurements of target and reference stars made at a given epoch, plus those measurements made shortly thereafter with orthogonal orientation of the baseline vector. The time interval between orthogonal measurements is chosen randomly within a range of a few days.

2.1. Orange Peel Scan Model

With regard to grid observations, in its present stage SIM has a greater degree of operating flexibility that its predecessor all-sky space astrometric mission Hipparcos. SIM is free to survey the geometry of the sky with essentially only a restriction on sun and earth avoidance. This is in sharp contrast to Hipparcos, which used a great circle scanning law particularly so that unmonitored systematic effects in the instrument could be identified over a relatively short (<12 hr) time period. Because SIM maintains common metrology references (both optical fiducial and laser frequency) for both the internal and external metrology systems, for the purposes of this work we assume that drifts of metrology components do not effect the observables produced by the system. This property frees SIM to scan the

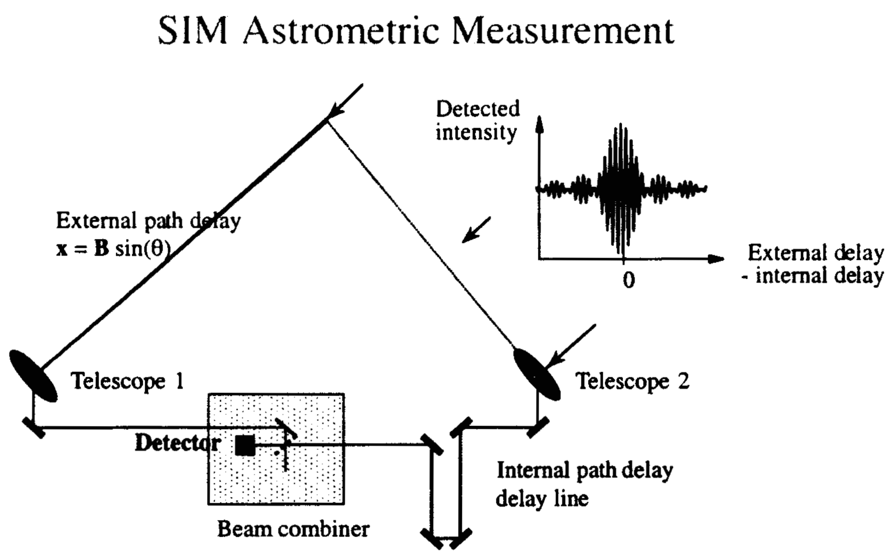

Figure 1. The SIM instrument does not directly measure the angular separation between stars, but the projection of each star direction vector onto the interferometer baseline vector by measuring the pathlength delay of starlight as it passes through the two arms of the interferometer. The peak of the interference pattern occurs when the internal path delay equals the external path delay.

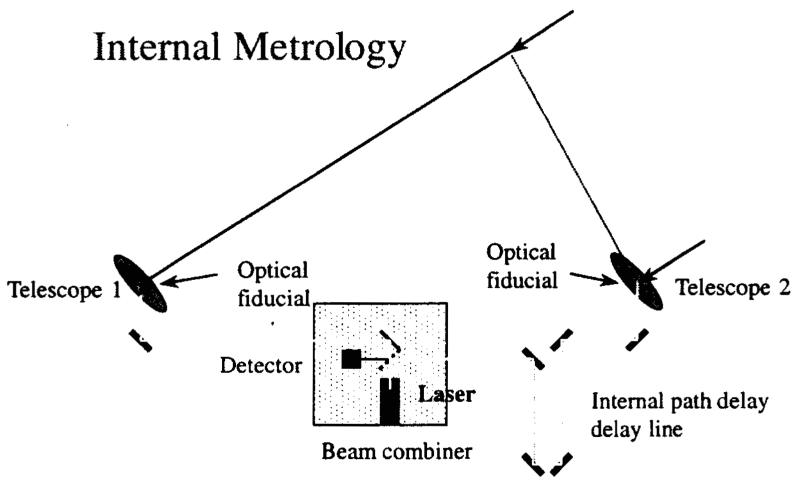

Figure 2. SIM makes the pathlength delay measurement by a combination of internal metrology measurements to determine the distance the starlight travels through the two arms of the interferometer and a measurement of the white light stellar fringe to find the point of equal pathlength. This operation requires a non–negligible integration time to accumulate enough photons to measure the stellar fringe position. As a result, the baseline vector is not stationary over this time period as its absolute length and orientation are time–varying. This conflicts with the requirement that a single baseline vector measures a set of stars. Laser gauge measures internal delay (adjusted by delay line, sensed by fringe detector). Laser path retraces starlight path from combiner to telescopes.

sky in virtually any method that is deemed appropriate, without having to tailor the global coverage geometry to solve for systematic effects.

This freedom may imply that SIM can integrate required grid observations into the normal routine of science observations. However, it may well be that the grid will have to be observed in periodic dedicated campaigns. At present this issue is poorly understood, and remains a topic for future study.

Formally, input to the grid astrometric estimation process consists of an input catalog of grid object astrometric parameters and a measurement set (such as described above). The measurement set is used to compute a refined set of astrometric parameters for the objects represented in the measurement set, and refined instrumental parameters pertaining to the measurement sequence. The refinement of these parameters is accomplished by computing a differential correction vector that is the least-squares solution to a large set of delay difference equations. This differential correction vector is added to the astrometric and instrument model parameters, and the entire process is repeated until the system becomes stable, or until the average parameter correction falls below some a priori expectation based on the measurement uncertainty properties. In practice the system is seen to converge to a stable solution after only a few (fewer than ten) iterations.

3. REGULARIZATION OF THE BASELINE

One of the important mission objectives is to accurately determine the directions to a grid of a stars, improving *a priori* knowledge of these relative directions by nearly three orders of magnitude. Because the accuracy with which these objectives are to be met is so great, not only is the star direction vector is unknown, but the interferometer baseline vector must also be estimated in an *a posteriori* manner since the knowledge provided by on-board attitude determination is several orders of magnitude inadequate. A consequence of this is that in order to generate a consistent set of equations from Eq.(1), multiple measurements of each star with different baselines orientation must be made, and dually multiple star measurements must be made for each baseline. The concept of a tile measurement refers to this later requirement.

Since some of the astrometric targets will be very dim, however, it is not possible for the science interferometer to track the fringes and compensate for the OPD variations in real time. As a result, the fringes associated with the science target will be washed out due to uncontrolled motions of the instrument. The adopted solution in these cases is to use the precise attitude information obtained from two other interferometers and construct a delay tracking signal that will be fed to the science interferometer's delay line in an open-loop fashion. This is called pathlength feed-forward. An analogous problem has to do with the pointing of the science interferometer collectors which must also be adjusted to correct for the uncontrolled attitude changes of the instrument. The solution to this problem is similar to the delay case, and is called angle feed-forward.

Precision astrometry requires knowledge of the baseline orientation to the same order of precision as the astrometric measurement. To achieve this, a minimum of three interferometers are required. Two interferometers acquire and lock on bright "guide" stars (s_{g1}, s_{g2}), keeping track of the directions to these stars, and hence also of the (uncontrolled) rigid-body motions of the instrument. A third interferometer switches between science targets (s_1, s_2, $\cdots$), measuring projected angles between them. An external metrology system keeps track of the flexible-body motions of the instrument by measuring changes in the baseline vectors of the three interferometers. The final result is obtained by linking the results from the three interferometers and the external metrology system.

4. DESCRIPTION OF THE INTERFEROMETER

In the current SIM design all three interferometers have a different baseline. In each arm, the collectors of the three interferometers are constrained to point to their respective targets through a common fiducial. Each fiducial consists of a double-corner-cube assembly, such that the vertices of the corner-cubes coincide, with one corner-cube being used for the three internal metrology systems, and the other for external metrology.

External metrology measures relative orientation of science and guide baselines, allows accurate transfer of attitude information from guides to science interferometer, provides long integration time for faint stars (see Fig. 3). Science interferometer stabilized by commanding its delay line.

Baseline is determined in frame of metrology reference structure, as determined by star tracker. The attitude information is used to stabilize the science interferometer by commanding its optical delay line (see Fig. 4). Because the a priori baseline vector is only known to arcsec accuracy through on-board attitude information, the interferometer baseline vector must also be estimated in an a posteriori manner in addition to the astrometric parameters. A consequence of this is that in order to generate a consistent set of equations from which to determine the astrometric parameters, multiple measurements of each star with different baseline orientations must be made, and dually multiple star measurements must be made with each baseline.

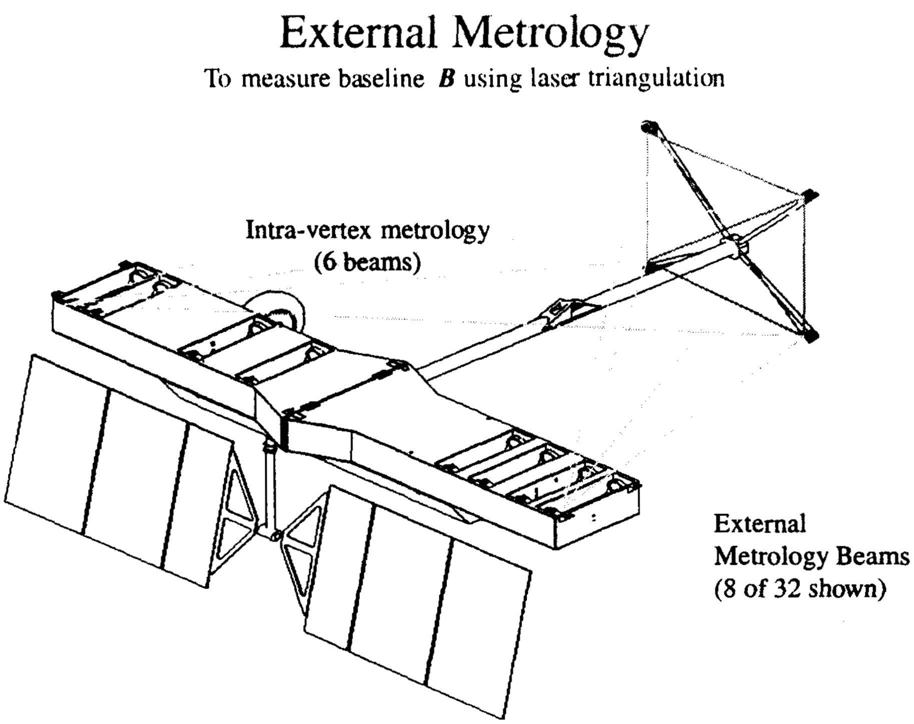

Figure 3. External metrology measures relative orientation of science and guide interferometers baselines.

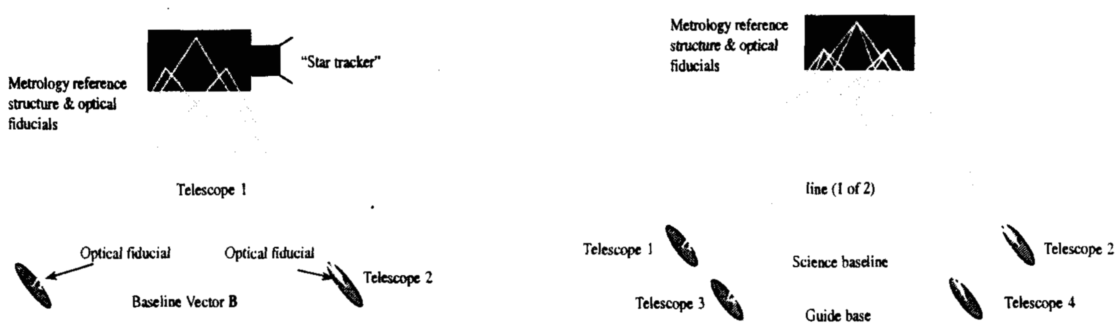

Figure 4. Baseline is determined in frame of metrology reference structure, as determined by star tracker.

4.1. Expected Stability of the Baseline

It is expected that the magnitude of the baseline's length changes $\epsilon(t, t_0)$ will be on the order of 10 μm over the time of a tile observation $\sim$ 1 hr:

$$\max_{\Delta t \sim 1\,\mathrm{hr}} |\epsilon(t, t_0)| \leq \frac{10\ \mu m}{10\ \mathrm{m}} \sim 10^{-6}\ \mathrm{rad}. \tag{2}$$

In addition to this the small attitude changes are due to uncompensated errors in spacecraft's three-dimensional motions may amount to about 30 arcseconds:

$$\max_{\Delta t \sim 1\,\mathrm{hr}} |\Delta\omega(t)| \leq 30 \text{ as} \sim 1.5 \times 10^{-4} \text{ rad}. \tag{3}$$

To the second order in small attitude variations, $\omega^\mu(t)$, we parameterize the instantaneous interferometer's baseline, $b^\epsilon(t)$, as follows:

$$b^\epsilon(t) = b(t_0)\Big(1 + \epsilon(t)\Big)\Big(\delta^\epsilon_\lambda + \omega^\mu(t)\,\epsilon^\epsilon_{\mu\lambda} + \frac{1}{2!}\omega^\mu(t)\omega^\nu(t)\,\epsilon^\epsilon_{\mu\rho}\epsilon^\rho_{\nu\lambda} + \mathcal{O}(\omega^3)\Big)n^\lambda(t_0), \tag{4}$$

where we have used the following notations:

- the greek letters $\alpha, \beta, ...$ running from 1 to 3, thus any vector may be given as follows: $\vec{a} = (a_1, a_2, a_3) \stackrel{\text{def}}{=} a^\lambda$;
- $b(t_0)$, $n^\lambda(t_0)$ are the initial baseline length and orientations of the guide interferometer;
- $\epsilon(t) = \Big(b(t) - b(t_0)\Big)/b(t_0)$ is the time-varying readings of the external metrology, $\epsilon(t_0) \equiv 0$;
- $\omega^\mu(t)$ is the vector of a small attitude changes in the baseline orientation for the interferometer, $\omega^\mu(t_0) \equiv 0$.
- we used the following convention for the cross vector product: $[\vec{\omega} \times \vec{a}]^\alpha \equiv \epsilon^\alpha_{\mu\lambda}\,\omega^\mu a^\lambda$, where $\epsilon_{\alpha\mu\lambda}$ is a fully anti-symmetric pseudo-tensor: $\epsilon_{\alpha\mu\lambda} = -\epsilon_{\mu\alpha\lambda} = \epsilon_{\mu\lambda\alpha} = -\epsilon_{\alpha\lambda\mu}$ and $\epsilon_{123} = 1$.

4.2. Expressions for the interferometric delays

This allows us to write the delays for all three interferometers (i.e. the two guides – ($\mathbf{g1}, \mathbf{g2}$) and one science – $\mathbf{s}$) in the following form:

$$d(t) = k(t) + \Big(\vec{b}(t) \cdot \vec{s}(t_0)\Big), \tag{5}$$

where $k(t)$ is the time-varying calibration term of the interferometer (i.e. the drifting "zero-point"). Note that at this point we assume that vector $\vec{s}$ does not change during t he observation of a tile. This restriction may be easily lifted and we will address this issue in a later studies.

Combing expressions Eqs.(4)-(5) one may form the delay equations. Thus, to the second order in $\omega^\lambda(t)$ one obtains the following expressions for the time-varying delays for the science and guide interferometers:

$$\begin{aligned} d_{\mathbf{s}}(t) &\equiv k_{\mathbf{s}}(t) + b_{\mathbf{s}}(t_0)\Big(1 + \epsilon_{\mathbf{s}}(t)\Big)\,n^\lambda_{\mathbf{s}}(t_0)s^\epsilon_{\mathbf{s}}(t_0)\times \\ &\times \Big[\delta_{\epsilon\lambda} + \omega^\mu_{\mathbf{s}}(t)\,\epsilon_{\epsilon\mu\lambda} + \frac{1}{2}\omega^\mu_{\mathbf{s}}(t)\omega^\nu_{\mathbf{s}}(t)\,\epsilon_{\epsilon\mu\rho}\epsilon^\rho_{\nu\lambda} + \mathcal{O}(\omega^3_{\mathbf{s}})\Big]. \end{aligned} \tag{6}$$

$$\begin{aligned} d_{\mathbf{gA}}(t) &\equiv k_{\mathbf{gA}}(t) + b_{\mathbf{gA}}(t_0)\Big(1 + \epsilon_{\mathbf{gA}}(t)\Big)\,n^\lambda_{\mathbf{gA}}(t_0)s^\epsilon_{\mathbf{gA}}(t_0)\times \\ &\times \Big[\delta_{\epsilon\lambda} + \omega^\mu_{\mathbf{gA}}(t)\,\epsilon_{\epsilon\mu\lambda} + \frac{1}{2}\omega^\mu_{\mathbf{gA}}(t)\omega^\nu_{\mathbf{gA}}(t)\,\epsilon_{\epsilon\mu\rho}\epsilon^\rho_{\nu\lambda} + \mathcal{O}(\omega^3_{\mathbf{gA}})\Big]. \end{aligned} \tag{7}$$

where we introduced the following notations: capital letters of Latin alphabet (`A,B,C,...`) denote the two guide interferometers and take only two values: `A,B,...= 1,2`; subscript "s" denotes the science interferometer, while "gA" stays for the $\mathtt{A}^{\mathrm{th}}$ guide interferometer.

Taking into account that, because of the flexible body motions, the rate of the attitude drifts of the guide interferometers is different from that of the science interferometer, we may write:

$$\omega^\mu_{\mathbf{gA}}(t) = \omega^\mu_{\mathbf{s}}(t) + \Delta\omega^\mu_{\mathbf{sgA}}(t), \qquad \Delta\omega^\mu_{\mathbf{gA}}(t) \sim \omega^2_{\mathbf{s}}(t). \tag{8}$$

Due to the same reason all the interferometers will be miss-aligned at the beginning of the observations. We define the contribution of this misalignment vector, $\omega^\mu_{0\mathbf{gA}}(t_0)$, to the initial baseline orientation of $\mathtt{A}^{\mathrm{th}}$ guide interferometer as given below:

$$n^\lambda_{\mathbf{gA}}(t_0) = n^\lambda_{\mathbf{s}}(t_0) + \epsilon^\lambda_{\mu\pi}\omega^\mu_{0\mathbf{gA}}(t_0)n^\pi_{\mathbf{s}}(t_0) + \frac{1}{2!}\omega^\mu_{0\mathbf{gA}}(t_0)\omega^\nu_{0\mathbf{gA}}(t_0)\epsilon^\lambda_{\mu\rho}\epsilon^\rho_{\nu\pi}n^\pi_{\mathbf{s}}(t_0) + ... \tag{9}$$

4.3. Equation for the Attitude Vector

Subtracting the initial conditions from the time-varying delays tracked by the guide interferometers, Eq.(eq:bg1), we obtain the equation that determines the instantaneous change in the science interferometer's baseline orientation:

$$\begin{aligned}
\Big[\omega^\mu_{\mathsf{s}}(t)\,\epsilon_{\mu\lambda\epsilon} \quad &+ \quad \Big(\frac{1}{2}\omega^\mu_{\mathsf{s}}(t)\omega^\nu_{\mathsf{s}}(t)+\omega^\mu_{\mathsf{s}}(t)\omega^\nu_{\mathsf{sgA}}(t_0)\Big)\,\epsilon_{\epsilon\mu\rho}\epsilon^\rho_{\nu\lambda}+\mathcal{O}\Big(\omega^3_{\mathsf{s}}(t)\Big)\Big]\,n^\lambda_{\mathsf{s}}(t_0)s^\epsilon_{\mathsf{gA}}(t_0) = \\
&= \frac{\Delta d_{\mathsf{gA}}(t)-\Delta k_{\mathsf{gA}}(t)}{b_{\mathsf{gA}}(t_0)\Big(1+\epsilon_{\mathsf{gA}}(t)\Big)} - \epsilon_{\mathsf{gA}}(t)\,n_{\mathsf{s}\lambda}(t_0)s^\lambda_{\mathsf{gA}}(t_0) - \Big[\delta\omega^\mu_{\mathsf{sgA}}(t)+\epsilon_{\mathsf{gA}}(t)\omega^\mu_{\mathsf{sgA}}(t_0)\Big]\epsilon_{\epsilon\mu\lambda}n^\lambda_{\mathsf{s}}(t_0)s^\epsilon_{\mathsf{gA}}(t_0), \quad (10)
\end{aligned}$$

where we defined the temporal variation of the measured delay for the guide interferometers, $\Delta d_{\mathsf{gA}}(t)$, and the temporal variation in the constant term, $\Delta k_{\mathsf{gA}}(t)$, as given below:

$$\begin{aligned}
\Delta d_{\mathsf{gA}}(t) &= d_{\mathsf{gA}}(t,t_0)-d_{\mathsf{gA}}(t_0), \qquad \Delta d_{\mathsf{g1}}(t_0)=0; \quad (11)\\
\Delta k_{\mathsf{gA}}(t) &= k_{\mathsf{gA}}(t)-k_{\mathsf{gA}}(t_0), \qquad \Delta k_{\mathsf{gA}}(t_0)=0. \quad (12)
\end{aligned}$$

Thus, we have obtained the system of equations to determine the attitude changes of the science interferometer. On may see that this system is underdetermined, in a sense that is is only two equations to determine the three components of the attitude vector. This is why only two out of three components of the attitude drift vector $\omega^\mu_{\mathsf{s}}(t)$ may be determined this way. We call the undetermined component - the unobservable roll.

4.4. Science Interferometer's Delay Equation

A solution to the set of equations, Eq.(10), may be obtained in the iterative way. In consideration of brevity we will not be presenting it here. However, we will present the final solution for the science interferometer's instantaneous delay. Thus, this delay was obtained with the help of solution for attitude matrix, $\omega^\mu_{\mathsf{s}}(t)$, and equation (6) in the following form:

$$\begin{aligned}
d_{\mathsf{s}}(t) \quad &= \quad k_{\mathsf{s}}(t_0)+\Delta k_{\mathsf{s}}(t)+b_0\cdot\Big\{\Big(1+\epsilon_{\mathsf{s}}(t)\Big)(\vec{n}_0\cdot\vec{s}_j)+b_0\cdot\epsilon^{\mathsf{AB}}\left(\vec{n}_0\cdot[\vec{g}_{\mathsf{A}}\times\Delta\vec{\omega}_{\mathsf{sgA}}(t)]\right)\cdot\frac{(\vec{n}_0\cdot[\vec{g}_{\mathsf{B}}\times\vec{s}_j])}{(\vec{n}_0\cdot[\vec{g}_1\times\vec{g}_2])}\Big\} - \\
&- \quad b_0\cdot\Big\{\epsilon^{\mathsf{AB}}\,p_{\mathsf{gA}}(t)\cdot(\vec{n}_0\cdot\vec{g}_{\mathsf{A}})\frac{(\vec{n}_0\cdot[\vec{g}_{\mathsf{B}}\times\vec{s}_j])}{(\vec{n}_0\cdot[\vec{g}_1\times\vec{g}_2])}+\frac{1}{2}\Big[\epsilon^{\mathsf{AB}}\,p_{\mathsf{gA}}(t)\cdot(\vec{n}_0\cdot\vec{g}_{\mathsf{A}})\cdot[\vec{n}_0\times\vec{g}_{\mathsf{B}}]\Big]^2\cdot\frac{(\vec{s}_j\cdot[\vec{g}_1\times\vec{g}_2])}{(\vec{n}_0\cdot[\vec{g}_1\times\vec{g}_2])^3}+ \\
&\qquad + \quad \epsilon^{\mathsf{AB}}\,p_{\mathsf{gA}}(t)\cdot\left(\vec{n}_0\cdot[\vec{g}_{\mathsf{A}}\times\vec{\omega}_{0\mathsf{gA}}]\right)\frac{(\vec{n}_0\cdot[\vec{g}_{\mathsf{B}}\times\vec{s}_j])}{(\vec{n}_0\cdot[\vec{g}_1\times\vec{g}_2])}+ \\
&\qquad + \quad \epsilon^{\mathsf{AB}}\,(\vec{n}_0\cdot\vec{g}_{\mathsf{A}})\cdot\epsilon^{\mathsf{CD}}\,p_{\mathsf{gC}}(t)\cdot(\vec{n}_0\cdot\vec{g}_{\mathsf{C}})\cdot\Big([\vec{n}_0\times\vec{\omega}_{0\mathsf{gA}}]\cdot[\vec{n}_0\times\vec{g}_{\mathsf{D}}]\Big)\frac{(\vec{n}_0\cdot[\vec{g}_{\mathsf{B}}\times\vec{s}_j])}{(\vec{n}_0\cdot[\vec{g}_1\times\vec{g}_2])^2} - \\
&\qquad - \quad \alpha_{\mathsf{s}}(t)\cdot\epsilon^{\mathsf{AB}}\Big([\vec{n}_0\times\vec{\omega}_{0\mathsf{gA}}]\cdot[\vec{n}_0\times\vec{g}_{\mathsf{A}}]\Big)\cdot\frac{(\vec{n}_0\cdot[\vec{g}_{\mathsf{B}}\times\vec{s}_j])}{(\vec{n}_0\cdot[\vec{g}_1\times\vec{g}_2])} \quad +\mathcal{O}\Big(\omega^{[3]}_{\mathsf{s}}(t);\omega^2_{0\mathsf{A}};\epsilon^2_{\mathsf{gA}}(t)\Big)\Big\} \qquad (13)
\end{aligned}$$

where $\epsilon^{\mathsf{AB}}=-\epsilon^{\mathsf{BA}}$ is anti-symmetric pseudo-tensor, normalized as $\epsilon^{12}=1$. Thus, $\epsilon^{\mathsf{AB}}\ell_{\mathsf{A}}p_{\mathsf{B}}\equiv\sum^{1,2}_{A,B}\epsilon^{\mathsf{AB}}\ell_{\mathsf{A}}p_{\mathsf{B}}=\ell_1p_2-\ell_2p_1$. The quantity $p_{\mathsf{gA}}(t)$ characterizes the pathlength feed-forward signal (instrumental drifts) and has the form:

$$p_{\mathsf{gA}}(t)=\Big(1+\epsilon_{\mathsf{s}}(t)-\epsilon_{\mathsf{gA}}(t)\Big)\cdot\frac{\Delta d_{\mathsf{gA}}(t)-\Delta k_{\mathsf{gA}}(t)}{d_{\mathsf{gA}}(t_0)-k_{\mathsf{gA}}(t_0)}-\epsilon_{\mathsf{gA}}(t) \qquad (14)$$

We also used the following notations:

- $\vec{b}_0=b_0\cdot\vec{n}_0$ – initial science baseline estimate (length, b_0, and orientation, $\vec{n}_0$);
- $\vec{g}_1,\vec{g}_2$ – the unit vectors for the two guide stars;
- $d_{\mathsf{s}}(t), d_{\mathsf{gA}}(t)$ – instantaneous interferometric delays;

$k_{0\mathbf{s}}, k_{0\mathbf{gA}}$	–	constant part of calibration terms for the interferometers at the beginning of observations;
$\vec{\omega}_{0\mathbf{gA}}$	–	initial miss-alighment of the $\mathtt{A}^{\mathrm{th}}$ guide interferometer baseline's orientation relative to that of the science interferometer's baseline;
$\Delta\vec{\omega}_{\mathbf{gA}}(t)$	–	contribution of the temporal drift of the $\mathtt{A}^{\mathrm{th}}$ guide interferometer's orientation relative to the science interferometer, (taken care by the external metrology);
$\alpha_{\mathbf{s}}(t)$	–	unobservable roll of the science interferometer averaged for j^{th} star.

5. ASTROMETRIC MODELING FOR SIM

It is expected that in the wide-angle mode, SIM will reach a design accuracy of 4 μas. Moreover, over a narrow field of view the relative accuracy is better, and SIM is expected to achieve an accuracy of 1 μas. In this mode, SIM will search for planetary companions to nearby stars, by detecting the astrometric 'wobble' relative to a nearby ($\leq 1°$) reference star. The expected proper motion accuracy is $\sim$2 μas yr^{-1}, corresponding to a transverse velocity of 10 m s^{-1} at a distance of 1 kpc.

Now we are in the position to characterize the instrumental contributions to the astrometric sensitivity of the future observations. To do this, we form a differential astrometric measurement, $\vec{n}_0\cdot\big(\vec{s}_j-\vec{s}_k\big)$. Thus with the help of expression (13) we have the following result:

$$
\begin{aligned}
\vec{n}_0\cdot\Big(\vec{s}_j-\vec{s}_k\Big) \;=\;& \frac{\langle d_{\mathbf{s}}\rangle_j-\langle d_{\mathbf{s}}\rangle_k}{b_0}-\frac{\langle\Delta k_{\mathbf{s}}\rangle_j-\langle\Delta k_{\mathbf{s}}\rangle_k}{b_0}-\Big(\langle\epsilon_{\mathbf{s}}\rangle_j\cdot(\vec{n}_0\cdot\vec{s}_j)-\langle\epsilon_{\mathbf{s}}\rangle_k\cdot(\vec{n}_0\cdot\vec{s}_k)\Big)-\\
&-\;\epsilon^{\mathtt{AB}}\left(\big(\vec{n}_0\cdot[\vec{g}_{\mathtt{A}}\times\langle\Delta\vec{\omega}_{\mathtt{A}}\rangle_j]\big)\cdot\frac{(\vec{n}_0\cdot[\vec{g}_{\mathtt{B}}\times\vec{s}_j])}{(\vec{n}_0\cdot[\vec{g}_1\times\vec{g}_2])}-\big(\vec{n}_0\cdot[\vec{g}_{\mathtt{A}}\times\langle\Delta\vec{\omega}_{\mathtt{A}}\rangle_k]\big)\cdot\frac{(\vec{n}_0\cdot[\vec{g}_{\mathtt{B}}\times\vec{s}_k])}{(\vec{n}_0\cdot[\vec{g}_1\times\vec{g}_2])}\right)+\\
&+\;\epsilon^{\mathtt{AB}}\,(\vec{n}_0\cdot\vec{g}_{\mathtt{A}})\left(\langle p_{\mathtt{A}}\rangle_j\cdot\frac{(\vec{n}_0\cdot[\vec{g}_{\mathtt{B}}\times\vec{s}_j])}{(\vec{n}_0\cdot[\vec{g}_1\times\vec{g}_2])}-\langle p_{\mathtt{A}}\rangle_k\cdot\frac{(\vec{n}_0\cdot[\vec{g}_{\mathtt{B}}\times\vec{s}_k])}{(\vec{n}_0\cdot[\vec{g}_1\times\vec{g}_2])}\right)+\\
+\;\frac{1}{2}\Bigg(\Big\langle\Big[\epsilon^{\mathtt{AB}}\,p_{\mathtt{A}}(t)\cdot(\vec{n}_0\cdot\vec{g}_{\mathtt{A}})\cdot[\vec{n}_0\times\vec{g}_{\mathtt{B}}]\Big]^2\Big\rangle_j\cdot&\frac{(\vec{s}_j\cdot[\vec{g}_1\times\vec{g}_2])}{(\vec{n}_0\cdot[\vec{g}_1\times\vec{g}_2])^3}-\Big\langle\Big[\epsilon^{\mathtt{AB}}\,p_{\mathtt{A}}(t)\cdot(\vec{n}_0\cdot\vec{g}_{\mathtt{A}})\cdot[\vec{n}_0\times\vec{g}_{\mathtt{B}}]\Big]^2\Big\rangle_k\cdot\frac{(\vec{s}_k\cdot[\vec{g}_1\times\vec{g}_2])}{(\vec{n}_0\cdot[\vec{g}_1\times\vec{g}_2])^3}\Bigg)+\\
&+\;\epsilon^{\mathtt{AB}}\,(\vec{n}_0\cdot[\vec{g}_{\mathtt{A}}\times\vec{\omega}_{0\mathtt{A}}])\left(\langle p_{\mathtt{A}}\rangle_j\cdot\frac{(\vec{n}_0\cdot[\vec{g}_{\mathtt{B}}\times\vec{s}_j])}{(\vec{n}_0\cdot[\vec{g}_1\times\vec{g}_2])}-\langle p_{\mathtt{A}}\rangle_k\cdot\frac{(\vec{n}_0\cdot[\vec{g}_{\mathtt{B}}\times\vec{s}_k])}{(\vec{n}_0\cdot[\vec{g}_1\times\vec{g}_2])}\right)+\\
+\;\epsilon^{\mathtt{AB}}\,(\vec{n}_0\cdot\vec{g}_{\mathtt{A}})\cdot\epsilon^{\mathtt{CD}}\,(\vec{n}_0\cdot\vec{g}_{\mathtt{C}})\cdot\Big([\vec{n}_0\times\;\vec{\omega}_{0\mathtt{A}}]\cdot[\vec{n}_0\times\vec{g}_{\mathtt{D}}]\Big)&\left(\langle p_{\mathtt{C}}\rangle_j\cdot\frac{(\vec{n}_0\cdot[\vec{g}_{\mathtt{B}}\times\vec{s}_j])}{(\vec{n}_0\cdot[\vec{g}_1\times\vec{g}_2])^2}-\langle p_{\mathtt{C}}\rangle_k\cdot\frac{(\vec{n}_0\cdot[\vec{g}_{\mathtt{B}}\times\vec{s}_k])}{(\vec{n}_0\cdot[\vec{g}_1\times\vec{g}_2])^2}\right)-\\
-\;\epsilon^{\mathtt{AB}}\Big([\vec{n}_0\times\vec{\omega}_{0\mathtt{A}}]\cdot[\vec{n}_0\times\vec{g}_{\mathtt{A}}]\Big)&\left(\langle\alpha_{\mathbf{s}}\rangle_j\cdot\frac{(\vec{n}_0\cdot[\vec{g}_{\mathtt{B}}\times\vec{s}_j])}{(\vec{n}_0\cdot[\vec{g}_1\times\vec{g}_2])}-\langle\alpha_{\mathbf{s}}\rangle_k\cdot\frac{(\vec{n}_0\cdot[\vec{g}_{\mathtt{B}}\times\vec{s}_k])}{(\vec{n}_0\cdot[\vec{g}_1\times\vec{g}_2])}\right)+\mathcal{O}\Big(\omega^{[3]}_{\mathbf{s}}(t);\omega^2_{0\mathtt{A}};\epsilon^2_{\mathbf{g}\mathtt{A}}(t)\Big)
\end{aligned}
$$

where small letters of Latin alphabet `(j,k,...)` denote the science stars observed in the tile and are running `j,k,...` = `1,2,..., N`. Also,

$\vec{s}_j, \vec{s}_k$;	–	the unit vectors for j^{th} and k^{th} science stars;
$\langle d_{\mathbf{s}}\rangle_j, \langle\Delta d_{\mathbf{gA}}\rangle_j$	–	measured science interferometer's delay and temporal change in the guide's delay for j^{th} star;
$\langle\Delta k_{\mathbf{s}}\rangle_j, \langle\Delta k_{\mathbf{gA}}\rangle_j$	–	contribution of a temporal drift in the calibration term to the measurements for j^{th} star;
$\langle\epsilon_{\mathbf{s}}\rangle_j, \langle\epsilon_{\mathbf{gA}}\rangle_j$	–	contribution of the beseline's length variation to the measurements for j^{th} star;
$\langle\Delta\vec{\omega}_{\mathbf{gA}}\rangle_j$	–	contribution of the temporal drift of the $\mathtt{A}^{\mathrm{th}}$ guide interferometer's orientation relative to the science interferometer, averaged for j^{th} star (taken care by the external metrology);

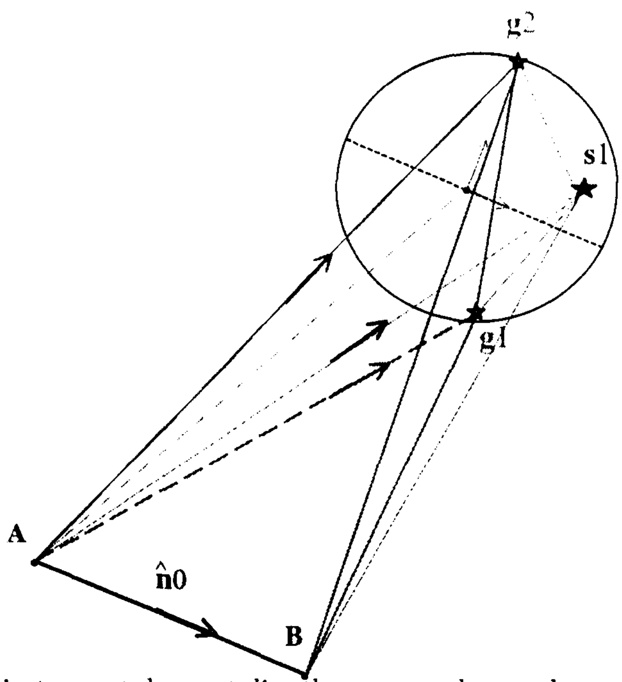

Figure 5. The SIM instrument does not directly measure the angular separation between stars.

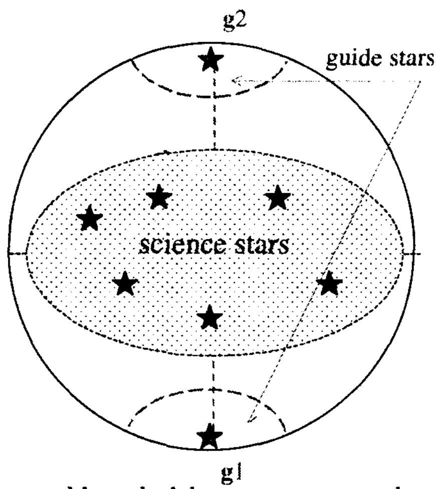

Figure 6. SIM makes the pathlength delay measurement by a combination of internal.

$\langle p_A \rangle_j$ – pathlength feed–forward signal (instrumental drifts) averaged for j^{th} star;
$\langle \alpha_s \rangle_j$ – unobservable roll of the science interferometer averaged for j^{th} star.

6. SUMMARY, CONCLUSIONS AND FUTURE PLANS

This memo is intended to serve several purposes. The first is to introduce the reader to the concept of the SIM astrometric grid, and its role and utility in the SIM mission. The second is to document the status, structure, and function for the suite of grid simulation tools under development by the SIM project in general, and by the SIM science team in particular. The third is to document the results obtained with this tool suite thus far, and finally the fourth is to indicate the future directions for this simulation development effort. The set of software described herein serves as the kernel of a powerful numerical capability to perform complicated system, instrument, and mission performance studies where the figure of merits are derivable from SIM astrometric performance. Several critical questions have already been addressed, and many more issues are presently or will soon be under study.

One major source of potential difficulty for grid observations and reductions is astrophysical jitter on the grid objects. For the work described herein grid objects are assumed to be astrometrically ideal (their kinematics are restricted to linear motion and annual parallactic displacement). However, SIM intentionally probes objects on astrometric scales where object dynamics are expected to be important. Examples of significant stellar dynamics with astrometric effects are undetected binary companions, massive planets, gravitational microlensing by intervenining bodies, and starspots. A major motivation in developing these simulation tools is to assess the grid performance implications of astrophysical effects. Assessing the impacts of such astrophysical effects on grid performance will be the focus of simulation activity in the next six months.

ACKNOWLEDGMENTS

This work was performed by the Jet Propulsion Laboratory, California Institute of Technology, under contract with the National Aeronautics and Space Administration.

REFERENCES

1. L. Lamport, *LaTeX A Document Preparation System*, Addison-Wesley, Reading, 1994.
2. A. Eisenberg, *Guide to Technical Editing*, Oxford University, New York, 1992.
3. A. Gelman, J. B. Carlin, H. S. Stern, and D. B. Rubin, *Bayesian Data Analysis*, Chapman & Hall, London, 1995.
4. N. Metropolis, A. W. Rosenbluth, M. N. Rosenbluth, A. H. Teller, and E. Teller, "Equations of state calculations by fast computing machine," *J. Chem. Phys.* **21**, pp. 1087–1091, 1953.
5. S. F. Gull, "Developments in maximum-entropy data analysis," in *Maximum Entropy and Bayesian Methods*, J. Skilling, ed., pp. 53–71, Kluwer Academic, Dordrecht, 1989.
6. K. M. Hanson, "Introduction to Bayesian image analysis," in *Image Processing*, M. H. Loew, ed., *Proc. SPIE* **1898**, pp. 716–731, 1993.